Journal of Electrical Engineering & Technology (2019) 14:701–710
https://doi.org/10.1007/s42835-019-00122-z

ORIGINAL ARTICLE

Influence of Inter-turn Short-Circuit Fault Considering Loop Current on Electromagnetic Field of High-Speed Permanent Magnet Generator with Gramme Ring Windings

Hongbo Qiu[1] · Xifang Zhao[1] · Cunxiang Yang[1] · Yi Ran[1] · Yanqi Wei[1]

Received: 8 October 2018 / Revised: 11 January 2019 / Accepted: 14 January 2019 / Published online: 5 February 2019

Abstract
As a kind of emergency power supply in military field, the high-speed permanent magnet generator (HSPMG) has attracted wide attention to its healthy condition. The loop current (LC) of the inter-turn short-circuit (ITSC) fault seriously endangers the generator unit operation stability and power supply reliability. In order to study the influence of pulsating magnetic field produced by LC on the electromagnetic field, the two-dimensional finite element model (FEM) of the 117 kW, 60000 rpm HSPMG is established. By comparing calculation result and test data, the accuracy of the model is verified. The field-circuit coupling method is used to reveal the change mechanism of magnetic field symmetry when ITSC fault occurs. By comparing the spatial distribution of the air-gap flux density, the relationship among the spatial distribution of the air-gap flux density, the elliptical rotating magneto-motive force (MMF) and the current phase angle is determined. The variation of the amplitude of the air-gap flux density space harmonic under different fault degree is studied, and the fault characteristics of ITSC fault are obtained, which provides a reference for ITSC fault diagnosis and fault degree identification. In addition, the research also laid a theoretical foundation for the next analysis of the loss and temperature field.

Keywords Air-gap flux density · High-speed permanent magnet generator · Inter-turn short circuit · Loop current · Space harmonic

1 Introduction

The high-speed permanent magnet generator (HSPMG) has the advantages of small volume, high reliability, high efficiency, small moment of inertia and fast dynamic response [1–3]. It has a good application prospect in the fields of aerospace, vacuum pump and flywheel energy storage [4, 5]. It is attracting more and more researchers' attention.

In order to reduce the stator core loss and external rectifier loss of the generator, it is necessary to minimize the operating frequency at a given rotating speed. Therefore, the number of poles chosen by the HSPMG is usually 2. If HSPMG adopts conventional winding, the stator end winding will be overlong. Especially when the pole numbers is 2, the length of the stator end windings will even be the same as the stator straight line winding. In addition, when the generator runs at a high speed, its frequency will exceed the first natural frequency [6]. When the rotor is overlong, the mechanical strength of the rotor is decreased, and the rotor will be deformed. However, the Gramme ring windings can effectively shorten the rotor overall length for better stiffness under high-speed rotation [7]. The Gramme ring windings are shown in Fig. 1a. One side of the Gramme ring winding is embedded in the stator core slot, and the other side is placed on the back of the stator yoke.

The ITSC fault of the stator winding is one of the common electrical faults, which accounts for about 30–40% of

✉ Xifang Zhao
zhaoxifang1993@163.com

Hongbo Qiu
qiuhongbohrb@163.com

Cunxiang Yang
yangcx77777@163.com

Yi Ran
yiranjob@163.com

Yanqi Wei
weiyanqi92@163.com

[1] Department of School of Electric and Information Engineering, Zhengzhou University of Light Industry, Zhengzhou, China

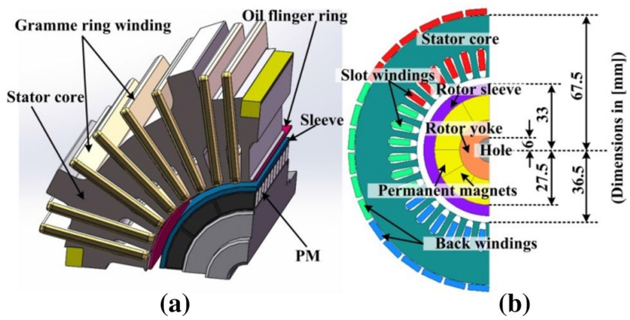

Fig. 1 **a** The structure of the HSPMG. **b** The two-dimensional FEM of the HSPMG

all faults [8]. In addition, the fault coil will induce a large short circuit LC when the ITSC fault occurs. This large short circuit LC causes the machine local temperature to rise and the insulation of the coils to deteriorate, eventually leading to more and more turns being short-circuited due to further insulation failure. Therefore, to prevent the expansion of the fault caused by the ITSC, it is necessary to study the ITSC fault.

In recent years, many scholars have done a lot of research on ITSC fault from various perspectives. The finite element method, the multiple-coupled circuit model based on winding function approach and magnetic equivalent circuit model are adopted to simulate ITSC fault model [9–12]. For rotor ITSC fault model, a new method to model the ITSC fault by a single set of equations is proposed in [13]. The novel analytical expressions are proposed for calculation of faulty permanent magnet (PM) motor inductances from healthy machine parameters in [14], and the results of fault studies help to find a signature of inter-turn fault in PM motors. In [15], a permanent magnet synchronous machine (PMSM) ITSC fault diagnosis is explored through impedance estimation and a discernment procedure is proposed for the ITSC and eccentricity faults which exhibit similar dynamic impedance behavior. In addition, the influences of the ITSC fault current needs to be considered during the design process [16]. Qiu and Yu studied and analyzed the influence of the ITSC fault considering the LC on permanent magnet synchronous motor losses, temperature fields [17] and electromagnetic fields [18]. It is worth mentioning that no similar study on the ITSC faults of the HSPMG with Gramme ring windings has been found in many literatures.

In this paper, the field-circuit coupling method is used to study the ITSC faults of the HSPMG with Gramme ring windings, taking into account the influence of pulsating magnetic field produced by the LC on the electromagnetic field. The research is carried out to study the influence of pulsating magnetic field around the fault slot on the magnetic field symmetry, air-gap flux density waveform and space harmonic amplitude of air-gap flux density. The research reveals the mechanism of magnetic field symmetry change, and determines the key factors affecting the air-gap flux density variation. And the fault characteristics of the ITSC are obtained, which provides a reference for the ITSC fault diagnosis and fault degree discrimination of the HSPMG. Furthermore, the next work will focus on the HSPMG loss and temperature field when the ITSC fault occurs,and the study laid a theoretical foundation for future research.

Table 1 The parameters of the HSPMG

Basic parameters	Value	Basic parameters	Value
Rated power (kW)	117	Stator outer diameter (mm)	135
Rated voltage (V)	670	Stator inner diameter (mm)	72
Pole number	2	Rotor outer diameter (mm)	66
Rotor type	PM	Core length (mm)	275
Frequency (Hz)	1000	Slot number	36
winding connection type	Y	Number of turns per slot	2

2 Parameters and Models of the Generator

2.1 Parameters and Models

In this paper, an 117 kW, 60,000 rpm HSPMG is investigated. Due to the small size of the high speed machines, the rotor space is limited. The rotor of the HSPMG is designed as a slender structure with 66 mm outer diameter. The permanent magnet adopts radial magnetization and it is mounted on the rotor yoke surface in an axially segmented way. The axially segmented is designed to reduce the eddy current loss. The high speed of the HSPMG leads to a great rotor surface linear velocity. It means that the rotor surface has great centrifugal force. Therefore, it is necessary to add a sleeve on the rotor surface to protect the permanent magnet. The material of sleeve is high-strength austenitic steel (50Mn18Cr5) with 0.5% C content, 18% Mn content, 5% Cr content, 0.5% Si content and so on, whose relative permeability is 1, and bulk conductivity is 1.31×10^6 S/m. In addition, the stator adopts a closed cavity oil cooling mode to increase the heat dissipation of Gramme ring winding and stator core. The basic parameters of the HSPMG are shown in Table 1. Based on the actual structure of the prototype, the two-dimensional FEM of the HSPMG is established, as shown in Fig. 1b. The FEM of the ITSC fault is shown in Fig. 2a. i_f is the LC, as shown in Fig. 2b and the region C of Fig. 3. In addition, when the ITSC fault occurs, the contact resistance is only considered and the resistance variation caused by temperature rise is not considered in this paper.

In order to simplify computational problems in electromagnetic field analysis, three hypotheses are made in this paper [19]:

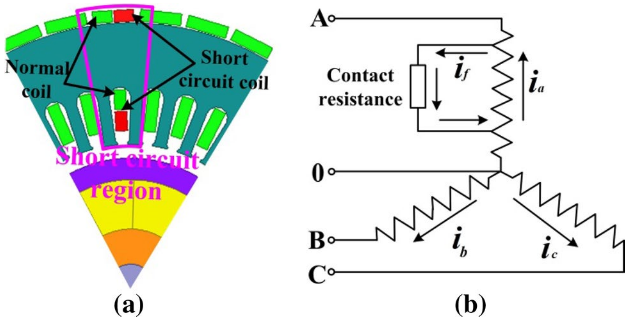

Fig. 2 **a** FEM of ITSC fault, **b** equivalent circuit diagram of ITSC fault

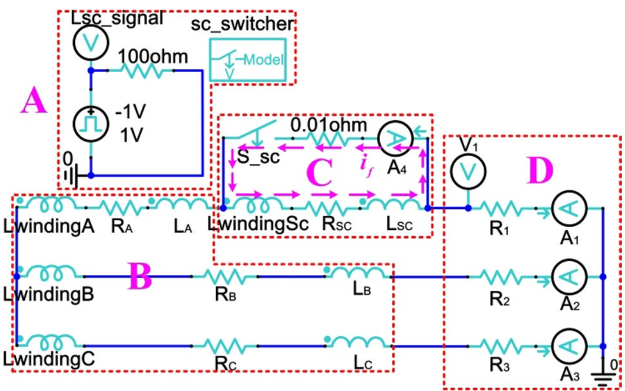

Fig. 3 External circuit of HSPMG

1. It is assumed that the magnetic field is uniformly distributed along the axial direction in the analysis of two-dimensional transient field. It means that current density vector $\boldsymbol{J}$ and magnetic potential vector A only have the component in the z-direction, $\boldsymbol{J} = \boldsymbol{J}_Z$, $\boldsymbol{A} = \boldsymbol{A}_Z$.
2. Materials are isotropic. The permeability of the material is constant and the variation of the permeability with the change of the temperature is ignored.
3. The influence of displacement current is assumed to be ignored. It is considered that the electromagnetic field of the generator is a nonlinear constant electromagnetic field.

Based on the above assumptions and electromagnetic field theory, the boundary value equation of generator two-dimensional transient electromagnetic field is established by $\boldsymbol{A}_Z$ in this paper [20]:

$$\begin{cases} \Omega : \frac{\partial^2 A_z}{\partial x^2} + \frac{\partial^2 A_z}{\partial y^2} = -\mu J_z + \mu\sigma \frac{\partial A_z}{\partial t} \\ \Gamma_1 : A_z = 0 \\ \Gamma_2 : \frac{1}{\mu_1}\frac{\partial A_z}{\partial n} - \frac{1}{\mu_2}\frac{\partial A_z}{\partial n} = J_s \end{cases},$$

where is Ω the calculation region, A_z and J_z are the magnetic vector potential and the source current density in the z-axial component, respectively, J_s is the equivalent face current density of the PM, σ is the conductivity, Γ_1 is the parallel boundary condition, Γ_2 is the PM boundary condition, and μ_1 and μ_2 are relative permeability values.

In this paper, the electromagnetic field of the HSPMG is analyzed by the field-circuit coupling method. The external circuit is shown in Fig. 3. In Fig. 3, region A is the switch S_sc control circuit model, which causes the switch close after the generator starts 4 ms. Region B is the non-fault equivalent circuit model of the HSPMG stator three phase windings. Region C is equivalent circuit model of fault windings. Region D is load.

2.2 Experimental Testing and Data Comparison

The HSPMG prototype was tested to verify the correctness of the analysis results. The experimental test platform and the experiment equipment are shown in Fig. 4. The terminal voltage and the armature current are obtained when the generator is running at the speed of 6000, 8000 and 10,000 rpm, respectively. The experimental data and the finite element model calculated results are shown in Table 2. In Table 2, the terminal voltage is the amplitude of the phase voltage, and the armature current is the amplitude of the phase current.

From the data in Table 2, there is little difference by comparing the experimental data with the model calculation results. The maximum difference of the terminal voltage between the test data and the calculated results is 0.7 V, and the error is not more than 1.13%. And the maximum difference of the armature current between the test data and the calculated results is 0.3 A, and the error is not more than 1.34%. Through the above data, the accuracy of the finite element model has been verified.

Figure 5 shows the comparisons of the EMF waveforms obtained from the test and the finite element method. It can be seen that the EMF waveforms obtained from the two methods are in agreement. Due to the less harmonic content of the EMF, the waveform is almost sinusoidal.

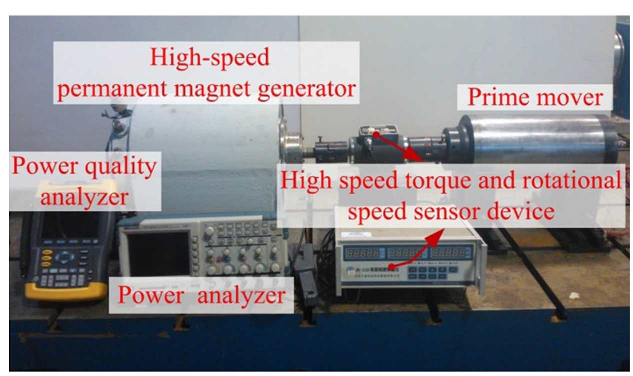

Fig. 4 Test platform of HSPMG

Table 2 Comparison of the test data and the finite element model calculated results

Speed (rpm)	Terminal voltage (V)		Error (%)	Armature current (A)		Error (%)
	Calculated results	Test data		Calculated results	Test data	
6000	39.9	39.6	0.75	14.5	14.4	0.69
8000	53.1	53.7	1.13	18.3	18.5	1.09
10000	65.8	65.1	1.06	22.4	22.1	1.34

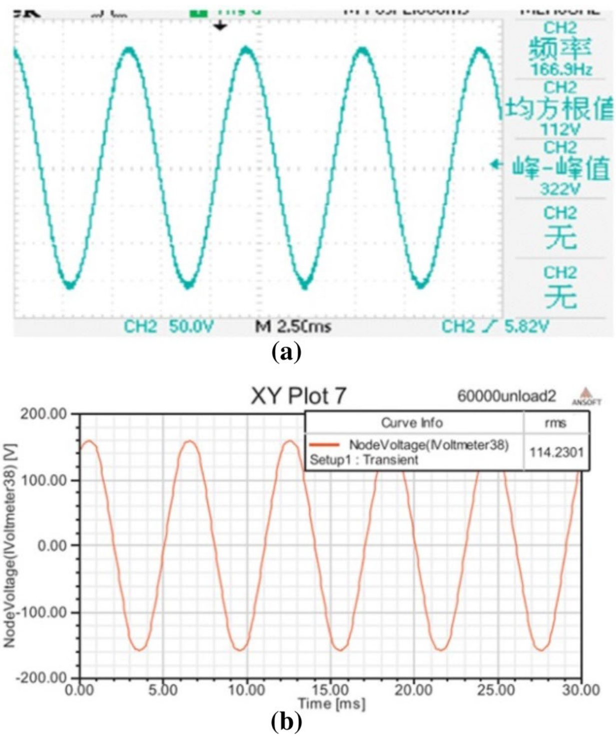

Fig. 5 **a** The test EMF waveform. **b** The finite element calculated EMF waveform

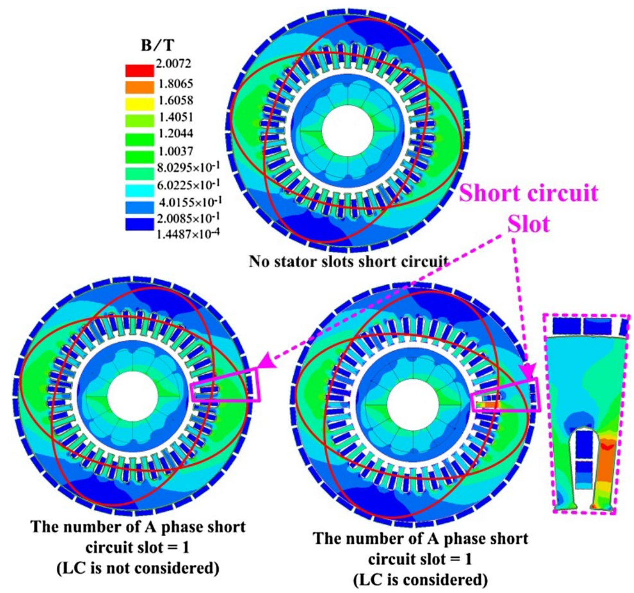

Fig. 6 The flux density distribution of HSPMG under normal and ITSC fault operation

3 Research and Analysis of the Influence of ITSC Fault on the Electromagnetic Field

As an energy conversion device, the electromagnetic field is the most important medium in the process of energy conversion. In the case of rated load of 3.6 Ohm, the distribution of the HSPMG magnetic field under normal operation condition and under the ITSC fault condition is compared and analyzed at the time of 0.012 s. Figure 6 shows the distribution of the flux density when A-phase short-circuits in one slot and each slot short-circuit in one turns, and the regular variation of flux density in the process of the ITSC fault is discussed. In order to facilitate analysis and comparison, the same scale is used.

Figure 6 shows that the distribution of the magnetic field is uniform under normal operation, and the symmetry of the magnetic field produced by the three-phase symmetrical winding is good. When the LC of the ITSC fault is not considered, the distribution of magnetic field is also uniform and symmetrical. In these two cases, the maximum value of the flux density appears in the stator yoke, and the value are both about 1.27T.

When the LC of the ITSC fault is considered, the magnetic field symmetry produced by the three-phase symmetrical winding is seriously destroyed. In addition, the uniformity of magnetic field distribution is also destroyed, and the local magnetic field of the HSPMG is significantly enhanced. In this case, the position of the maximum value of the magnetic flux density is transferred from the stator yoke of normal operation to the stator tooth of the fault slot. The maximum value of the magnetic flux density is about 2.01T, which is increased by 58.1% compared with that under normal operation. However, the stator material of the HSPMG is DW310-35 and the inflection point of magnetization curve is about 1.27T. Therefore, the magnetic field is obviously saturated when the LC of the ITSC fault is considered.

Through the finite element calculation, Fig. 7 shows the variation of the each phase currents before and after fault.

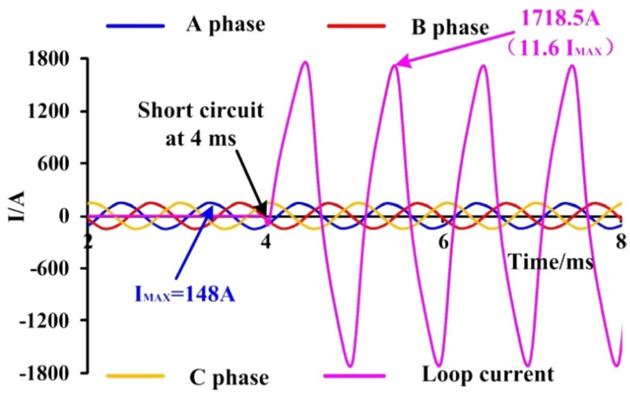

Fig. 7 The variation of the each phase currents before and after fault

The LC induced by the fault coil is about 11.6 times the normal winding current, and the maximum value can reach 1718.5A. The pulsating magnetic field generated by this large LC will surround the fault slot, which makes the magnetic field around the fault slot significantly enhanced and the magnetic field of the fault tooth is seriously saturated.

It can be seen that the LC of the ITSC fault is the main reason for the serious destroy of the magnetic field symmetry produced by the three-phase symmetrical winding. The LC also makes the magnetic field saturated and the core loss is increased. In addition, there are only two coils in each slot of HSPMG. The local heating caused by the large LC will greatly shorten the insulation life around the fault coil, and even destroy the whole slot coils in serious cases. Therefore, the next work will focus on the HSPMG loss and temperature field when the ITSC fault occurs.

4 Research and Analysis of Influence of ITSC on the Air-gap Flux Field of HSPMG

The air-gap magnetic field analysis is an important research content in mechanism analysis and feature extraction of generator internal electrical fault. In addition, when HSPMG under normal operation, the stator and rotor generate rotating magnetic fields respectively, and they are coupled in the air gap. Finally, it exists in the air gap in the form of synthetic rotating magnetic field, and the electromagnetic torque is generated to achieve energy transfer. Therefore, the internal fault of the HSPMG will inevitably affect the synthetic magnetic field. And it causes the air-gap flux density waveform distorted, which has a very adverse impact on the HSPMG. Therefore, it has a great significance to study and analyze the variation of the air-gap magnetic field before and after fault.

4.1 Comparison of Spatial Distribution of the Air-gap Flux Density

In the case of rated load of 3.6 Ohm, the air-gap flux density waveforms under normal operation condition and before and after fault is compared and analyzed at the time of 0.012 s. The air-gap flux density waveforms under different conditions are shown in Fig. 8.

In the ITSC fault region, the armature reaction of the HSPMG is weakened due to the reduction of winding turns in the fault region when the LC is not considered. The maximum value of the air-gap flux density is smaller than that of normal operation. When the LC is considered, the magnetic field generated by the LC leads to the magnetic enhancement of the armature reaction in the fault region. The maximum value of air gap magnetic density is about 1.11T, which is 3.26 times that under the normal operation and 4.29 times that under the ITSC fault without considering the LC. In addition, the tip of the air-gap flux density waveform coincides with the number of short circuit slots due to the effect of slotting effect, which significantly changes the spatial distribution of the air-gap flux density waveform.

In the non-fault region, the air-gap flux density is nearly equal to that of normal operation when the LC of the ITSC fault is not considered. When the LC of the ITSC fault is considered, the air-gap flux density is first lower than that under normal operation and then exceeds that of normal operation with the increase of mechanical angle. In the following the part 4.2 and 4.3, the reasons why the spatial

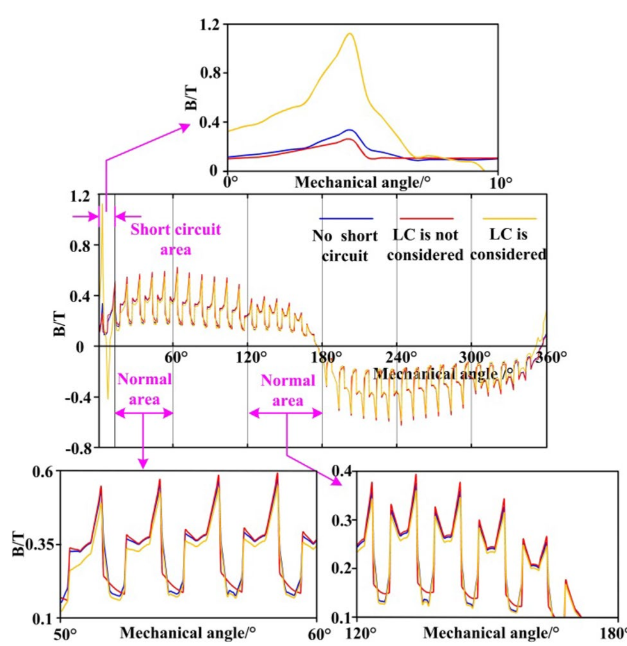

Fig. 8 The air-gap flux density waveforms under the normal operation and before and after fault

distribution of the air-gap flux density changes in the non-fault region will be explained.

4.2 Relationship Between the Spatial Distribution of the Air-gap Flux Density and the Current Phase Angle

The amplitude and phase angle of HSPMG output current will change when the ITSC fault occurs. Based on the Fourier decomposition principle, the current is decomposed under the normal and the ITSC fault operation. Figure 9 shows the current phase angle under different conditions intuitively. In addition, Table 3 further quantifies the relationship between the ITSC fault three-phase current phase angle and the normal three-phase current phase angle.

As can be seen from Fig. 9, the θ_{CA} under the ITSC fault is almost the same as that under the normal operation. Compared with that under the normal operation, the variation of the θ_{AB}, θ_{BC} are about 1° when the ITSC fault occurs. Therefore, the study of the current phase angle cannot be ignored.

As shown in Table 3, when the LC is not considered, the A-phase and C-phase lag those under the normal operation by 0.3° and 0.35° respectively, which causes the magnetic weakening of the armature reaction. The B-phase leads that under the normal operation by 0.69°, which causes the magnetic enhancement of the armature reaction. However, in the non-fault region, the magnetic enhancement of the armature reaction is nearly equal to the magnetic weakening of the armature reaction, which makes the air-gap flux density under the ITSC fault is nearly equal to that of normal operation.

When the LC is considered, the A-phase, B-phase and C-phase lag those under the normal operation by 2.76°, 0.9° and 1.55° respectively, which causes the magnetic weakening of the armature reaction. Therefore, in the non-fault region, the air-gap magnetic density under the ITSC fault is lower than that of the normal operation firstly.

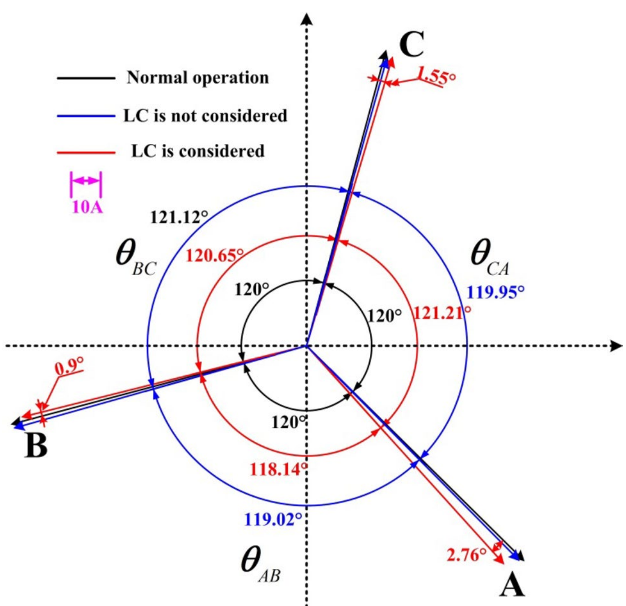

Fig. 9 The current phase angle of HSPMG under the normal and the ITSC fault operation

4.3 Relationship Between the Spatial Distribution of the Air-gap Flux Density and the Elliptical Rotating MMF

When the current flows through the stator winding, the MMF and magnetic field will be generated, and the magnetic field can be measured by the MMF. According to the knowledge of electric machinery, the fundamental wave MMF of each phase winding can be divided into two circular MMFs with equal amplitude and opposite displacement direction.

If the three-phase current flowing through the stator windings is positive-sequence (negative-sequence) current, the decomposed three reverse (forward) rotating MMFs will cancel each other, which leads to the fundamental wave synthetic MMF. The fundamental wave synthetic MMF is a circular rotating MMF with forward (reverse) shift. The circular rotating MMF wave is shown in Fig. 10a. The variation of the three-phase current before and after failure is shown in Fig. 11. As shown in Fig. 11, the ITSC fault causes the three-phase output current of the stator to be asymmetrical. Therefore, the positive-sequence current coexists with the negative-sequence current, and the forward rotating MMF coexist with the reverse rotating MMF.

It is assumed that the amplitudes of the forward and reverse rotating MMF are F_{1+} and F_{1-} respectively, θ_s is the angle of electricity on the stator. The three phase fundamental synthesis MMF:

$$f_1(\theta_s, t) = F_{1+}\cos\left(\omega t - \theta_s\right) + F_{1-}\cos\left(\omega t + \theta_s\right).$$

The transverse axis component of the fundamental synthesis MMF $\boldsymbol{F_1}$ is x, and the longitudinal axis component is y:

Table 3 The relationship between the ITSC fault three-phase current phase angle and the normal three-phase current phase angle

Type	LC is considered			LC is not considered		
	A	B	C	A	B	C
Lead	0°	0°	0°	0°	0.68°	0°
Lag	2.76°	0.9°	1.55°	0.3°	0°	0.35°

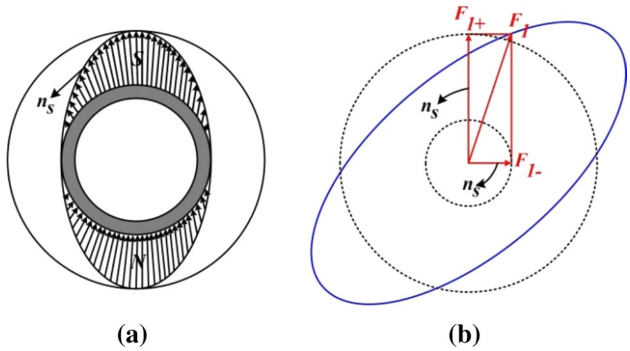

Fig. 10 **a** The circular rotating MMF. **b** The elliptical rotational MMF generated by asymmetric currents

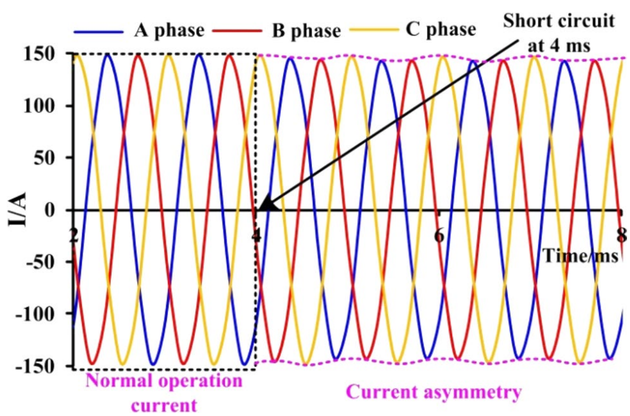

Fig. 11 The variation of the three-phase current before and after failure

$$\begin{cases} x = F_{1+}\cos\omega t\cos\theta_s + F_{1-}\cos\omega t\cos\theta_s = \left(F_{1+} + F_{1-}\right)\cos\omega t\cos\theta_s \\ y = F_{1+}\sin\omega t\sin\theta_s - F_{1-}\sin\omega t\sin\theta_s = \left(F_{1+} - F_{1-}\right)sin\omega t\sin\theta_s \end{cases}.$$

The relationship can be obtained

$$\frac{x^2}{a^2} + \frac{y^2}{b^2} = 1\ ,$$

where $a = (F_{1+} + F_{1-})\cos\theta_s$,$b = (F_{1+} - F_{1-})\sin\theta_s$.

$\boldsymbol{F}_{1+}$ and $\boldsymbol{F}_{1-}$, respectively represent the space vector of the forward and reverse rotating MMF. By combining $\boldsymbol{F}_{1+}$ and $\boldsymbol{F}_{1-}$ at different moments, it is known that the vector $\boldsymbol{F}_1$ of the fundamental synthesis MMF will be a rotating MMF with amplitude variation and non-constant velocity shift. As shown in Fig. 10b, the amplitude locus of the MMF is an ellipse. The armature reactions produced by fundamental armature MMF will also change. Therefore, when the LC of the ITSC fault is considered, the air-gap flux density exceeds that of under normal operation with the increase of mechanical angle.

Through the above analysis, it can be seen that the pulsating magnetic field produced by the LC significantly changes the spatial distribution of the air-gap flux density in the fault region. The variation of the armature reaction caused by current phase angle and the elliptical rotating MMF caused by asymmetric current are the main reasons for the variation of the air-gap flux density distribution in non-fault region. In addition, the variation of the air-gap magnetic field will lead to the increase of electromagnetic torque ripple and other phenomena, which will threaten the stable operation of the generator.

5 Research and Analysis of the Influence of ITSC Fault on the Air-gap Magnetic Field Space Harmonics

In an ideal state, the distribution of the electromagnetic field in the generator will be uniform and symmetrical, and the air-gap flux density waveform is approximately sinusoidal. The higher the sinusoidal degree of the air-gap flux density waveform is, the better the generator performance is. When the ITSC fault occurs, the space harmonics destroy the uniformity and symmetry of the air-gap magnetic field and reduce the sinusoidal degree of the air-gap magnetic density waveform. In addition, the harmonic magnetic field can generate eddy current losses in the sleeve of the rotor surface and cause heat. Not only the efficiency of the generator is reduced, but also the permanent magnet has the risk of demagnetization.

In order to compare and analyze the influence of fault degree on the spatial harmonics of the air-gap magnetic field, the air-gap flux density under the normal operation and the different fault degree is decomposed by using Fourier decomposition principle. The fundamental and harmonic amplitudes of the air-gap flux density are obtained, as shown in Fig. 12. In Fig. 12, the F presents the fundamental. In addition, due to the Y type connection of the generator winding, three and three multiples of the harmonics could not flow in the generator, so the 3th, 9th harmonics and so on could be ignored. On this basis, the variations of space harmonics under the ITSC fault are compared and analyzed, and the characteristics of the ITSC fault are explored.

As shown in Fig. 12, when the LC is not considered, the magnetic enhancement effect of the armature reaction is increased with the deepening of the fault degree. Therefore, the fundamental component of the air-gap flux density increases gradually with the deepening of the fault degree. When the LC is considered, the magnetic weakening effect of the armature reaction is increased with the deepening of the fault degree. Therefore, the fundamental component of the air-gap flux density is decreased gradually with the deepening of the fault degree.

In addition, the pulsating magnetic field generated by the LC surrounds the fault slot, which will affect the slot effect

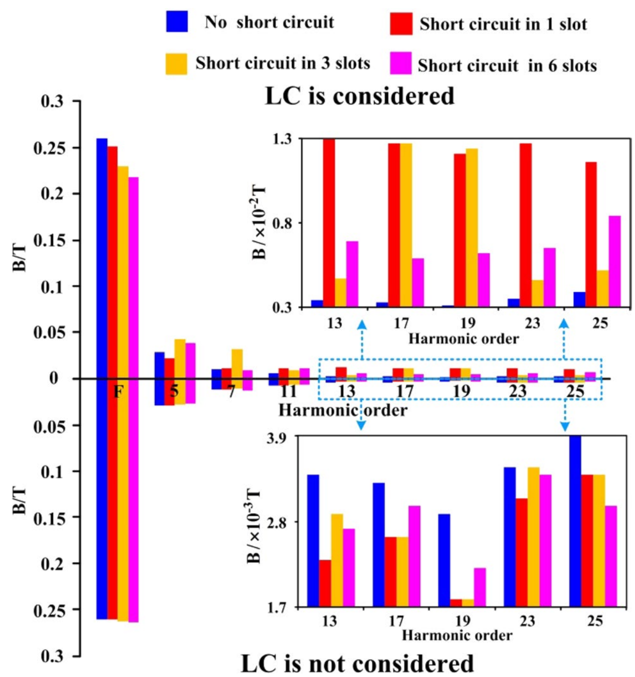

Fig. 12 The fundamental and harmonic amplitudes of the air-gap flux density

of the generator. Therefore, when the LC is considered, the higher harmonic components (such as 13th, 17th, 19th, etc.) of the air-gap flux density produced by slot effect under the different fault degree are obviously higher than those of under normal operation. However, when the LC is not considered, the higher harmonic components of the air-gap flux density produced by slot effect under the different fault degrees are lower or approximately equal to those of under normal operation.

The above is intuitive comparison and analysis of the harmonic components under different fault levels. Table 4 further quantifies the fundamental and harmonic amplitudes of the air-gap flux density under the different fault degree.

The ITSC fault of the stator winding is not easy to detect at the early stage. As shown in Table 4, when the stator winding is short-circuited in one slot, the higher harmonic components (such as 13th, 17th, 19th, etc.) of the air-gap flux density produced by slot effect are about four times as much as those of under normal operation. Therefore, the ITSC fault of stator winding can be identified in time by measuring the higher harmonic amplitude of air-gap magnetic density.

Without considering the LC, when the stator winding is short-circuited in 1 slot, 3 slots and 6 slots, the fundamental amplitude of the air-gap flux density is increased by 0.15, 0.77 and 1.46%, respectively compared with that under normal operation. Considering the LC, when the stator winding is short-circuited in 1 slot, three slots and six slots, the fundamental amplitude of the air-gap flux density is decreased by 3.3, 11.8 and 16.1%, respectively compared with those under normal operation. Therefore, the fault degree can be determined by measuring the fundamental amplitude of the air-gap magnetic density.

6 Conclusions

An 117 kW, 60,000 rpm high-speed permanent magnet generator (HSPMG) is taken as an example, the influence of the pulsating magnetic field around the fault slot on the magnetic field symmetry, the air-gap flux density waveform and the space harmonic amplitude of the air-gap flux density are studied. The conclusions are:

1. The LC of the ITSC fault is the main reason for the serious damage of the magnetic field symmetry. The pulsating magnetic field generated by the LC will surround the fault slot, which makes the magnetic field around the fault slot significantly enhanced. The position of the maximum value of the magnetic flux density is transferred from the stator yoke of the normal operation to the stator tooth of the fault slot. Taking this HSPMG as an example, the maximum value of the magnetic flux density is 2.01T under the ITSC fault considering the LC, which is increased by 58.1% compared with the normal operation. The magnetic field of the HSPMG is seriously saturated and the iron loss is increased.
2. The pulsating magnetic field produced by the LC is the primary cause for the variation of the air-gap flux den-

Table 4 The fundamental and harmonic amplitudes of the air-gap flux density under the different fault degrees

Harmonic orders	Normal operation	LC is considered			LC is not considered		
		One slot	Three slots	Six slots	One slot	Three slots	Six slots
F (T)	0.2612	0.2526	0.2303	0.2192	0.2616	0.2632	0.265
13th (T)	0.0034	0.0132	0.0047	0.0069	0.0023	0.0029	0.0027
17th (T)	0.0033	0.0127	0.0127	0.0059	0.0026	0.0026	0.003
19th (T)	0.0029	0.0121	0.0124	0.0062	0.0018	0.0018	0.0022
23th (T)	0.0035	0.0127	0.0046	0.0065	0.0031	0.0035	0.0034
25th (T)	0.0039	0.0116	0.0052	0.0084	0.0034	0.0034	0.003

sity spatial distribution in the fault region. The variation of the armature reaction caused by current phase angle and the elliptical rotating MMF caused by asymmetric current are the main reasons for the variation of the air-gap flux density distribution in non-fault region. In the fault area, the maximum value of the air-gap flux density reaches about 1.11T, which is 3.26 times that under the normal operation and 4.29 times that under the ITSC fault without considering the LC. In addition, when the LC is considered, the A-phase, B-phase and C-phase lag those of the normal operation by 2.76°, 0.9° and 1.55°, respectively, which causes the magnetic weakening of the armature reaction.

3. The pulsating magnetic field generated by the LC surrounds the fault slot, which will affect the higher harmonic components of the air-gap flux density produced by slot effect. When the LC is considered, the higher harmonic components (such as 13th, 17th, 19th, etc.) of the air-gap flux density produced by slot effect under the different fault degrees are obviously higher than those of under normal operation. Especially when the stator winding is short-circuited in 1 slot, the higher harmonic components of the air-gap flux density are about 4 times as much as those of under normal operation.
4. The ITSC fault of stator winding can be identified in time by measuring the higher harmonic amplitude of air-gap magnetic density. Considering the LC, when the stator winding is short-circuited in 1 slot, 3 slots and 6 slots, the fundamental amplitude of the air-gap flux density is decreased by 3.3, 11.8 and 16.1%, respectively compared with those under normal operation. Therefore, the fault degree can be determined by measuring the fundamental amplitude of the air-gap magnetic density.

Acknowledgements This work was supported in part by the National Natural Science Foundation of China under Grant 51507156, in part by the University Key Scientific Research Programs of Henan province under Grant 17A470005, in part by the Key R & D and Promotion Projects of Henan Province under Grant 182102310033, in part by the Doctoral Program of Zhengzhou University of Light Industry under Grant 2014BSJJ042, and in part by the Foundation for Key Teacher of Zhengzhou University of Light Industry.

References

1. Jang S-M, Koo M-M, Park Y-S, Choi J-Y, Lee S-H (2011) Characteristic analysis of permanent magnet synchronous machines under different construction conditions of rotor magnetic circuits by using electromagnetic transfer relations. IEEE Trans Magn 47(10):3665–3668
2. Duong M-T, Chun Y-D, Park B-G, Kim D-J, Choi J-H, HanH P-W (2017) Thermal analysis of a high speed induction motor considering harmonic loss distribution. J Electr Eng Technol 12:1503–1510
3. Zhang Y, McLoone S, Cao WP (2018) Electromagnetic loss modeling and demagnetization analysis for high speed permanent magnet machine. IEEE Trans Magn 54:8200405
4. Chen D, Feng M (2016) The influence of magnetic field on losses of high-speed permanent magnet motor. In: Proc 2016 IEEE Int Conf Mechatronics and Automation, Harbin, Heilongjiang, China, pp 27–31
5. Jeong K-I, Lee D-H, Ahn J-W (2018) Design and analysis of a high speed single-phase hybrid 4/4 poles SRM for hammer beaker application. J Electr Eng Technol 13(5):1978–1985
6. Li S, Li Y, Choi W, Sarlioglu B (2016) High speed electric machines—challenges and design considerations. IEEE Trans Transport Electr 2(1):2–13
7. Dong J, Huang Y, Jin L, Guo B, Lin H, Dong J, Cheng M (2014) HElectromagnetic and thermal analysis of open-circuit air cooled high-speed permanent magnet machines with gramme ring windings. IEEE Trans Magn 50:8104004
8. Li J, Wang D, Ma L, Jun qing (2011) The research of the inter-turn short circuit of the stator windings in doubly fed induction generator. Int Conf Electr Mach Syst 2011:1–4
9. Qing LJ, Dong W, Long H (2013) Study of rotor winding inter-turn short circuit fault in doubly fed induction generator based on current signal spectrum analysis. Int Conf Electr Mach Syst 66:789–792
10. Qing LJ, Long H, Dong W (2013) Rotor winding inter-turn fault analysis of doubly-fed induction generator based on negative sequence component. Int Conf Electr Mach Syst 56:785–788
11. Djurovic S, Williamson S, Renfrew A (2009) Dynamic model for doubly-fed induction generators with unbalanced excitation, both with and without winding faults. IET Electr Power Appl 3(3):171–177
12. Roshanfekr R, Jalilian A (2015) Analysis of rotor and stator winding inter-turn faults in WRIM using simulated MEC model and experimental results. Electr Power Syst Res 119:418–424
13. Naderi P, Shiri A (2017) Rotor/stator inter-turn short circuit fault detection for saturable wound-rotor induction machine by modified magnetic equivalent circuit approach. IEEE Trans Magn 53:8107013
14. Vaseghi B, Nahid-mobarakh B, Takorabet N, Meibody-Tabar F (2011) Inductance Identification and study of PM motor with winding turn short circuit fault. IEEE Trans Magn 47:978–981
15. Qi Y, Zafarani M, Akin B, Fedigan SE (2017) Analysis and detection of inter-turn short-circuit fault through extended self-commissioning. IEEE Trans Ind Appl 53(3):2730–2739
16. Dusek J, Arumugam P, Brunson C, Amankwah EK, Hamiti T, Gerada C (2014) Impact of slot/pole combination on inter-turn short-circuit current in fault-tolerant permanent magnet machines. IEEE Trans Magn 52:8102709
17. Qiu H, Wenfei Y, Tang B, Yang C, Zhao H (2017) Research on the influence of inter-turn short circuit fault on the temperature field of permanent magnet synchronous motor. J Electr Eng Technol 12(4):1566–1574
18. Qiu H, Wenfei Yu, Yuan S, Tang B, Yang C (2017) The influence of inter-turn short circuit fault considering loop current on the electromagnetic field of permanent magnet synchronous motor. COMPEL Int J Computa Math Elect Electron Eng 36(4):1028–1042
19. Li WL, Zhang XC, Cheng SK, Cao JC (2012) Thermal optimization for a HSPMG used for distributed generation systems. IEEE Trans Ind Electron 60:474–481
20. Zhang H, Zhang X, Gerada C, Li J (2015) Optimization on the tooth top shape of a high speed permanent magnetic generator. In Proc. 2015 IEEE International Magnetics Conference. Beijing, China. 11–15 May

Publisher's Note Springer Nature remains neutral with regard to jurisdictional claims in published maps and institutional affiliations.

Hongbo Qiu received the Graduation degree from the Harbin University of Science and Technology, Harbin, China, and the Ph.D. degree in electrical engineering from the same university in 2014. He has been with the Zhengzhou University of Light Industry, Zhengzhou, China, since 2014. His research interests include electromagnetic and thermal analysis on electrical machine, especially in permanent magnetic machines.

Xifang Zhao is pursuing the M.S. degree at the Zhengzhou University of Light Industry of China. His current research interests include electromagnetic analysis on high speed permanent magnet generator.

Cunxiang Yang received the M.S. degree from Southeast University of China, in 1996. He is currently a Professor with the College of Electrical and Electronic Engineering, Zhengzhou University of Light Industry, China. His research interests include the diagnosis of electric motors and the control of intelligent electrical apparatus.

Yi Ran received the M.S. degree from the Harbin University of Science and Technology, Harbin, China, in 2012. She has been with the Zhengzhou University of Light Industry, Zhengzhou, China, since 2014. Her research interests include research on electromagnetic and thermal analysis on electrical machine, particularly in superconducting machines.

Yanqi Wei is pursuing the M.S. degree at the Zhengzhou University of Light Industry of China. His current research interests include electromagnetic analysis on high speed permanent magnet generator.